Vol 16 No 1, January 2007
1009-1963/2007/16(01)/0001-05

Chinese Physics

© 2007 Chin. Phys. Soc.
and IOP Publishing Ltd

Rapid Communication

Effective-mass theory for coupled quantum dots grown on $(11N)$-oriented substrates*

Li Shu-Shen(李树深)† and Xia Jian-Bai(夏建白)

State Key Laboratory for Superlattices and Microstructures, Institute of Semiconductors, Chinese Academy of Sciences, Beijing 100083, *China*

(Received 3 September 2006; revised manuscript received 8 September 2006)

The electronic structures of coupled quantum dots grown on $(11N)$-oriented substrates are studied in the framework of effective-mass envelope-function theory. The results show that the all-hole subbands have the smallest widths and the optical properties are best for the (113), (114), and (115) growth directions. Our theoretical results agree with the available experimental data. Our calculated results are useful for the application of coupled quantum dots in photoelectric devices.

Keywords: coupled quantum dots, effective-mass theory, electronic structures
PACC: 7320D, 7115B, 7125W

1. Introduction

Coupled quantum dots (CQDs) formed in high-index GaAs substrates are currently a subject of intense interest. The electron and hole energies are strongly influenced by the strong zero-dimensional quantum confinement effect with a δ-function-like density of states.[1−7]

Nishi *et al*[8] reported that GaAs (311) is a better choice than GaAs (100) as a substrate for the growth of InGaAs QDs. Wang *et al*[9] investigated the laterally ordered, multi-layered arrays of InGaAs CQDs by photoluminescence as a function of high-index of GaAs substrates. High optical quality was demonstrated for the laterally ordered CQD arrays. GaAs (511)B was identified as the optimum high-index substrate for the growth of InGaAs/GaAs multi-layered CQDs, demonstrating a strong photoluminescence with a narrow full-width-at-half-maximum linewidth of 23 meV, despite the potential for misfit dislocations.[9]

Xia[10] gave an effective-mass formulation for a superlattice grown on $(11N)$-oriented substrates. It was found that, for a GaAs/AlGaAs superlattice, the hole subband structure and related properties were sensitive to orientation because of the large anisotropy of the valence band. The energy level positions for the heavy hole and the optical transition matrix elements for the light hole apparently changed with orientation.

We have studied the electronic structures, interband optical transition,[11] and intraband optical absorption[12] of InAs/GaAs CQDs grown on (100)-oriented substrates. In this letter, we will study the electronic structures of CQDs grown on $(11N)$-oriented substrates in the framework of effective-mass envelope-function theory.

2. Theoretical model

In our study, we choose the growth direction $(11N)$ as the x_3 direction of our coordinate system, and treat the CQDs as cylinders. In the x_3 direction, the height of the dots is L. In the direction perpendicular to $(11N)$, the radius of the CQDs is R. The schematic plot of the CQDs is the same as in Fig.1 of Ref.[9]. The potential energy of the electron and hole is

$$V_{\mathrm{e,h}}(\boldsymbol{r}) = \begin{cases} 0 & \text{for } |x_3| < L/2 \text{ and } x_1^2 + x_2^2 < R^2, \\ V_{\mathrm{e0,h0}} & \text{elsewhere,} \end{cases} \tag{1}$$

*Project supported in part by the National Natural Science Foundation of China (Grant Nos 60521001 and 60325416).
†E-mail: sslee@red.semi.ac.cn

where $\boldsymbol{r} = (x_1, x_2, x_3)$. $V_{\rm e0}$ and $V_{\rm h0}$ are the band offsets of the electron and hole, respectively. The electron envelope function equation is

$$H_{\rm e}\,\Psi_{\rm e} = E_{\rm e}\,\Psi_{\rm e}. \tag{2}$$

Equation (2) can be solved for the eigenvalues and eigenfunctions of the system by expanding $\Psi_{\rm e}$ in terms of normalized plane-wave states and diagonalizing the resultant matrix.[13] We assume that the electron wavefunctions have the following forms:

$$\Psi_{\rm e}(\boldsymbol{r}) = \frac{1}{\sqrt{L_1L_2L_3}}\sum_{nml} C_{nml}{\rm e}^{{\rm i}[(k_1+nK_1)x_1+(k_2+mK_2)x_2+(k_3+lK_3)x_3]} \tag{3}$$

with $K_1 = 2\pi/L_1$, $K_2 = 2\pi/L_2$, and $K_3 = 2\pi/L_3$. L_1, L_2, and L_3 are the periods along the x_1, x_2, and x_3 directions, respectively. For cylindrical CQDs, we take $L_1 = L_2$, and $n, m, l = 0, \pm1, \pm2, \ldots$. The matrix elements of Hamiltonian $H_{\rm e}$ in Eq.(2) for Eq.(3) can be written as

$$\frac{\hbar^2}{2m_{\rm e}^*}\delta(k_{1n}k'_{1n} + k_{2m}k'_{2m} + k_{3l}k'_{3l}) + (\delta - S_iS_j)V_{\rm e0}, \tag{4}$$

with

$$S_i = \begin{cases} \dfrac{L}{L_3} & \text{for } \ l = l', \\ \dfrac{\sin[\pi(l-l')L/L_3]}{\pi(l-l')} & \text{for } \ l \neq l', \end{cases} \tag{5}$$

$$S_j = \begin{cases} \dfrac{\pi R^2}{L_1^2} & \text{for } \ n = n' \ \text{ and } \ m = m', \\ \dfrac{R}{\lambda L_1}J_1(\lambda K_1 R) & \text{for } \ n \neq n' \ \text{ or } \ m \neq m', \end{cases} \tag{6}$$

where

$$\begin{aligned} &k_{1n} = (k_1 + nK_1), \quad k'_{1n} = (k_1 + n'K_1), \\ &k_{2m} = (k_2 + mK_2), \quad k'_{2m} = (k_2 + m'K_2), \\ &k_{3l} = (k_3 + lK_3), \quad k'_{3l} = (k_3 + l'K_3), \\ &\lambda = \sqrt{(n-n')^2 + (m-m')^2}, \end{aligned}$$

and $J_1(x)$ is the first-order Bessel function of x. δ is the δ-function given by

$$\delta = \begin{cases} 1 & \text{for } n = n' \text{ and } m = m' \text{ and } l = l', \\ 0 & \text{for } n \neq n' \text{ or } m \neq m' \text{ or } l \neq l'. \end{cases} \tag{7}$$

Therefore, we can calculate the electron energy levels in a vertical electric field from Eq.(4).

The hole effective mass Hamiltonian can be written as[10]

$$\begin{aligned} H_{\rm h} = \frac{\hbar^2}{2m_0^*}[&\gamma_1 k^2 + \gamma_2(Ak_1^2 + Bk_2^2 + Ck_3^2 + Dk_1k_2 \\ &+ Ek_1k_3 + Fk_2k_3) + \gamma_3(A'k_1^2 + B'k_2^2 + C'k_3^2 \\ &+ D'k_1k_2 + E'k_1k_3 + F'k_2k_3)] + V_{\rm h}, \end{aligned} \tag{8}$$

where γ_1, γ_2, and γ_3 are the Luttinger effective-mass parameters; m_0 is the free-electron mass. A, B, C, $\ldots$, E', and F' are 4×4 matrix.[10]

The hole envelope function equation is

$$H_{\rm h}\,\Psi_{\rm h} = E_{\rm h}\,\Psi_{\rm h}. \tag{9}$$

Using the normalized plane-wave expansion method,[13] we assume that the hole wavefunctions have the following forms:

$$\Psi_{\rm h}(\boldsymbol{r}_{\rm h}) = \frac{1}{\sqrt{L_1L_2L_3}}\sum_{nml}\begin{bmatrix} a_{nml} \\ b_{nml} \\ c_{nml} \\ d_{nml} \end{bmatrix}{\rm e}^{{\rm i}[(k_1+nK_1)x+(k_2+mK_2)y+(k_3+lK_3)z]}. \tag{10}$$

The matrix elements of Hamiltonian (8) for Eq.(10) can be written as

$$\frac{\hbar^2}{2m_0^*}[\gamma_1((k_{1n})^2+(k_{2m})^2+(k_{3l})^2)+\gamma_2(A(k_{1n})^2+B(k_{2m})^2+C(k_{3l})^2 + Dk_{1n}k_{2m}+Ek_{1n}k_{3l}+Fk_{2m}k_{3l})+\gamma_3(A'(k_{1n})^2+B'(k_{2m})^2+C'(k_{3l})^2 + D'k_{1n}k_{2m}+E'k_{1n}k_{3l}+F'k_{2m}k_{3l})]\delta+(\delta-S_iS_j)V_{\rm h0}\,. \quad (11)$$

Thus, the hole energy levels can be worked out from Eq.(11).

3. Results and discussion

For InGaAs, we take the material parameters given in Ref.[14]. The electron effective mass and Luttinger parameters are listed in Table 1. The band gaps of GaAs and InGaAs are 1.5177 eV and 816 meV, respectively. The conduction-band offset is assumed to be 65% of the band gap difference.

Table 1. The electron effective mass and Luttinger parameters for InGaAs.

$m_{\rm e}^*/m_0$	γ_1	γ_2	γ_3
0.043	11.01	4.18	4.84

For an isolated quantum dot and period CQDs, the electronic structures are divisive energy level structures and energy subband structures, respectively.

For the conduction band, the band structures are isotropic. The CQD conductive subband structures are independent of the growth direction. Figures 1(a) and 1(b) give the first two electron energy subbands as functions of CQD size along the growth direction and perpendicular to the growth direction, respectively. The solid and dotted lines correspond to the Γ and R points of the first Brillouin zone (see Fig.1 in Ref.[13]). In calculations, the periods of the CQDs are fixed at $L_1 = L_2 = L_3 = 20$ nm. As the sizes of the CQDs increase, from Fig.1 we can find that (i) electron energies decrease; (ii) the first energy band widths decrease monotonically; (iii) the second energy band widths increase at first and then decrease.

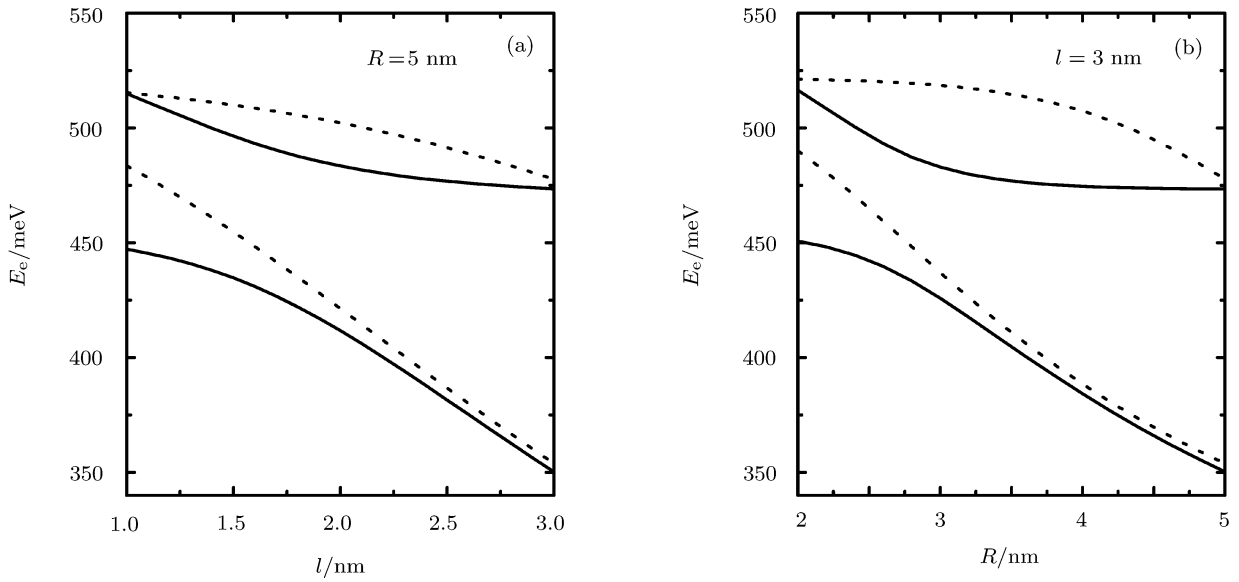


Fig.1. The first two electron energy subbands as functions of CQD size along the growth direction (a) and perpendicular to the growth direction (b), respectively. The solid and dotted lines correspond to the Γ and R points of the first Brillouin zone. The periods of the CQDs are $L_1 = L_2 = L_3 = 20$ nm.

The valence band near Γ is anisotropic. Many properties of superlattices,[10] quantum wires,[15] and CQDs are dependent on the growth direction. Figure 2(a) shows the first five hole energy subbands as functions of the growth direction $(11N)$ with CQD height $l = 3$ nm, radius $R = 5$ nm and periods $L_1 = L_2 = L_3 = 20$ nm. The solid and dotted lines correspond respectively to the Γ and R points of the first Brillouin zone (see Fig.1 in Ref.[13]). For the same CQD structure, from Fig.2(a) we find that (i) the first and third hole energy subbands (heavy-hole) have minimum for the (112) growth direction; (ii) the second, fourth and fifth hole subbands (light-hole) have minimum for the (113) growth direction; (iii) for $N \geq 4$, the hole subbands ascend slightly as N increases; (iv) for the (111) growth direction, the second and higher subbands have maximum; (v) for the (113), (114), and (115) growth directions, the all-hole subbands have the smallest widths, and the optical properties are the best. This is the first theoretical explanation of the experimental results in Refs.[8] and [9].

Figure 2(b) shows the first five hole energy subbands of spherical CQD as functions of the growth direction $(11N)$ with CQD radius $R = 5$ nm and periods $L_1 = L_2 = L_3 = 20$ nm. The solid and dotted lines correspond to the Γ and R points of the first Brillouin zone (see Fig.1 in Ref.[13]). This figure also shows that the optical properties are the best for the (113), (114), and (115) growth directions.

Using multi-band $\boldsymbol{k} \cdot \boldsymbol{p}$ model,[16] the calculated electronic structures will be somewhat different. Main conclusions will be the same as those using the single-band effective mass model. Including strain effects,[11] the heavy- and light-hole energy levels will be decreased and increased some what, respectively. The variation trends of the hole energy levels against the different growth direction are the same as those obtained by neglecting strain effects.

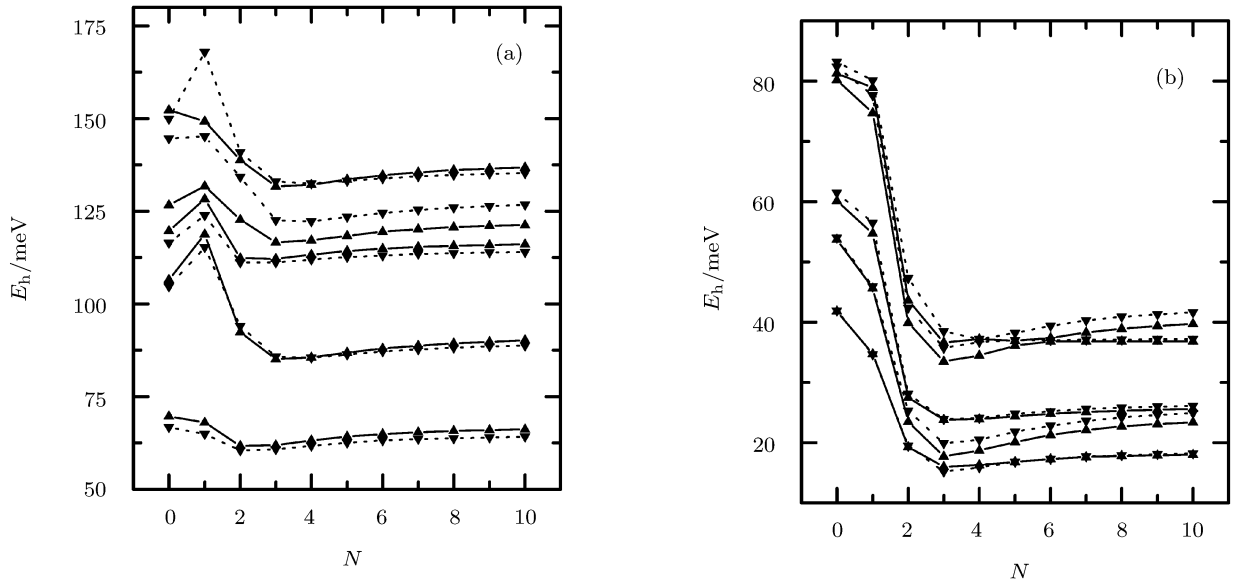


Fig.2. The first five hole energy subbands of columniform CQD with height $l = 3$ nm, radius $R = 5$ nm (a) and spherical CQD with radius $R = 5$ nm (b) as functions of the growth direction $(11N)$ with periods $L_1 = L_2 = L_3 = 20$ nm. The solid and dotted lines correspond to the Γ and R points of the first Brillouin zone.

In summary, our results show that the optical properties of CQD are best for the CQDs grown in the (113), (114), and (115) growth directions. This conclusion does not sensitively depend on the QD geometric shape, effective-mass model, and strain effects.

References

[1] Marzin J M, Gerard J M, Izrael A, Barrier D and Bastard G 1994 *Phys. Rev. Lett.* **73** 716

[2] Fafard S, Leno R, Leonard D, Merz J L and Petroff P M 1994 *Phys. Rev.* B **50** 8086

[3] Leonard D, Pond K and Petroff P M 1994 *Phys. Rev.* B **50** 11687

[4] Xie Q, Madhukar A, Chen P and Kobayashi N P 1995 *Phys. Rev. Lett.* **75** 2542

[5] Zhang H, Liu L and Liu J J 2007 *Acta Phys. Sin.* **56** 490(in Chinese)

[6] Xie W F 2006 *Chin. Phys.* **15** 203

[7] Grundmann M, Christen J, Ledentsov N N, Bohrer J, Bimberg D, Ruvimov S S, Werner P, Richter U, Gosele U, Heydenreich J, Ustinov V M, Egorov A Yu, Zhukov A E, Kop'ev P S and Alferov Z I 1995 *Phys. Rev. Lett.* **74** 4043

[8] Nishi K, Mirin R, Leonard D, Medeiros-Ribeiro G, Petroff P M and Gossard A C 1996 *J. Appl. Phys.* **80** 3466

[9] Wang Zh M, Mazur Y I, Seydmohamadi Sh, Salamo G J and Kissel H 2005 *Appl. Phys. Lett.* **87** 213105

[10] Xia J B 1991 *Phys. Rev.* B **43** 9856

[11] Li S S, Xia J B, Yuan Z L, Xu Z Y, Ge W K, Wang X R, Wang Y and Chang L L 1996 *Phys. Rev.* B **54** 11575

[12] Li S S and Xia J B 1997 *Phys. Rev.* B **55** 15434

[13] Cusack M A, Briddon P R and Jaros M 1996 *Phys. Rev.* B **54** 2300

[14] Vurgaftmana I and Meyer J R 2001 *J. Appl. Phys.* **89** 5815

[15] Li S S and Xia J B 1994 *Phys. Rev.* B **50** 8602

[16] Ng S T, Fan W J, Dang Y X and Yoon S F 2005 *Phys. Rev.* B **72** 115341